

INTRODUCING A NEW SCALING METHOD FOR NEAR-FAULT GROUND MOTIONS BASED ON THE ROOT-MEAN-SQUARE OF SPECTRAL RESPONSES

A. Yahyaabadi¹, M. Tehranizadeh¹

¹Department of Civil and Environmental Engineering, Amirkabir University of Technology
424 Hafez Ave, Tehran, Iran, 15875-4413
A.Yahyaabadi@aut.ac.ir, Dtehz@yahoo.com

Keywords: Nonlinear Dynamic Analysis, Near-Fault Ground Motions, Scaling Method, Seismic Demand, Collapse Capacity, Variability.

Abstract. *Assessment of the seismic performance of a structure often requires conducting nonlinear dynamic analyses under a set of ground motion records scaled to a specific level of intensity. Recent researches have demonstrated that pseudo spectral acceleration at the first mode period of vibration, $S_a(T_1)$, which is commonly used as the seismic intensity scaling index, may introduce a large scatter in the estimated seismic demands under near-fault pulse-like ground motions. Considering the need to provide more accurate estimation of seismic demands by using a smaller number of records, development of an improved scaling method that can reduce the variability in seismic demands becomes inevitable.*

In this paper, an improved intensity measure is developed based on the Root-Mean-Square (RMS) value of spectral responses, which is calculated over an appropriate period range. For this purpose, Incremental Dynamic Analyses (IDAs) are carried out for five generic frames of short to relatively long periods under 40 pulse-like earthquake records rotated to the fault-normal direction. Statistical study of the IDAs results is performed to determine the type of the response spectrum (i.e. pseudo acceleration, velocity or displacement) and the optimal period range for calculating the RMS value as the improved scaling method.

Statistical evaluation reveals that the RMS of pseudo spectral accelerations, $(S_a)_{rms}$, provides much superior results than RMS of spectral displacements, $(S_d)_{rms}$, and RMS of spectral velocities, $(S_v)_{rms}$. It is concluded that the optimal period range varies with the fundamental period of a structure, and that $(S_a)_{rms}$, if calculated over the optimal period range, can predict the seismic demands with the overall dispersions that are generally reduced by the relative amount of 14 percent with respect to those of $S_a(T_1)$. The newly proposed parameter can also reduce the dispersion in predicted collapse capacities of the frames by the relative amount of 24 percent compared to $S_a(T_1)$ on average.

1 INTRODUCTION

Performance Based Earthquake Engineering (PBEE) has received much attention in recent years as the new proficient method that can provide a quantitative basis in assessment of the seismic performance of structures. PBEE is a desirable concept and its implementation depends strongly on the ability to confidently estimate the probability that Engineering Demand Parameter (EDP), such as maximum storey drift, plastic hinge rotation and member force, exceeds a specific value. The probability that the EDP exceeds a specific value is a function of seismological random variables (such as magnitude and distance) and structural random variables (such as stiffness, strength, ductility and mass), and it is typically estimated through combining the results of Incremental Dynamic Analyses (IDAs) of a structure and seismic hazard analysis. In IDA, the intensity of each record is incremented after each inelastic dynamic analysis by using an intermediate quantity as the seismic intensity scaling index which is usually referred to as Intensity Measure (IM) [1].

The IM, as the seismic intensity scaling index, should represent those parameters of earthquake ground motions that strongly influence the structural responses, and it is required to introduce a small variability in EDP at any given IM level ($\sigma_{EDP|IM}$). A small variability is desirable because the standard error of sample mean of $\ln(EDP)$ for any specified IM level is equal to the ratio of the $\sigma_{EDP|IM}$ to the square root of n , where n is the number of earthquake records that have been sampled, and the sample mean of $\ln(EDP)$ is typically the first-order information used in quantifying the probabilistic seismic demand analysis [2].

Selecting the appropriate intensity measure for near-fault ground motions requires more accurate attention for special characteristics of this type of motions. In near-fault records influenced by forward directivity or fling step phenomena, most of the seismic energy from the rupture appears as a single coherent pulse-type motion. Ground motions having such a distinct pulse-like character generally arise at the beginning of the seismogram, and their effects tend to increase the long-period portion of the acceleration response spectrum. Studies have shown that for this type of motions, the maximum demand is a function of the ratio of the ground motion's pulse period, T_P , to the fundamental period of the structure [3]. With respect to this issue, the pseudo spectral acceleration measured at the first mode period of vibration, $S_a(T_1)$, which is commonly used as the IM in the performance-based earthquake engineering, cannot adequately predict the seismic demands imposed on structures by near-fault pulse-like ground motions [3], because it is not good representative for those parameters of near-fault earthquakes, such as pulse period, that affect the response of the structures.

The major shortcoming of $S_a(T_1)$, as the IM, is its inability in describing the effective frequency content of earthquakes at $T \neq T_1$. This weakness is more pronounced when pulse motions dominate the structural responses. The efficiency of $S_a(T_1)$ can be approximately improved by incorporating ε , shown to capture the average local spectral shape at T_1 , via a vector IM for ordinary earthquakes [4]. Nevertheless, pulse-like motions cannot be adequately characterized by the vector of $S_a(T_1)$ and ε , because their response spectra usually exhibit a sharp change, making it difficult to simply estimate spectral shape using $S_a(T_1)$ and local spectral shape at T_1 via epsilon [5, 6].

For near-fault earthquakes, Yang and Coworker have proposed intensity measures of Improved Effective Peak Acceleration (IEPA) for rigid systems, and Improved Effective Peak Velocity (IEPV) for medium to long period systems [7]. IEPA and IEPV have been respectively defined based on the average value of spectral accelerations and spectral velocities around their predominant peak. Whereas IEPA and IEPV have been developed based on the frequency characteristics of near-fault earthquakes, since these IMs are calculated over individual period ranges of records, and these period ranges are only defined based on the predo-

minant period of each response spectrum without any consideration of modal periods of a structure, they may introduce a large record to record variability [8]. It has been shown that the frequency content of earthquakes at a period range around the first mode period of a structure can describe the damaging effects of ground motions on the structure in a much better manner [8].

In this paper, an improved intensity measure is developed based on the Root-Mean-Square (RMS) value of spectral responses, calculated over an optimal period range, in order to reduce the variability in seismic demands under near-fault pulse-like ground motions. Based on the Incremental Dynamic Analyses (IDAs) of five frames of various heights under 40 near-fault pulse-like ground motions, it is shown that RMS of pseudo spectral accelerations, $(S_a)_{\text{rms}}$, provides much superior results than RMS of spectral velocities, $(S_v)_{\text{rms}}$, and RMS of spectral displacements, $(S_d)_{\text{rms}}$. All possible period ranges for calculating the RMS value are considered, and the optimal period range that can significantly reduce the overall variability in seismic demands obtained from IDAs is proposed. It is shown that the optimal period range is a function of the fundamental period of the structure, and that RMS of pseudo spectral accelerations, $(S_a)_{\text{rms}}$, calculated over the proposed period range, can considerably increase the accuracy of the seismic demand prediction with respect to $S_a(T_1)$.

2 STRUCTURAL SYSTEMS

Incremental dynamic analyses results of two-dimensional generic one-bay frames were used to develop the newly improved IM. The advantage of using the generic frames is that they do not represent a specific structure and thereby the results from analyses are not a function of a particular system. They are adequate to capture the global behavior of multi-bay frames and to evaluate the sensitivity of the results to various structural heights [9].

The generic frames used in this study consist of frames with number of stories, N , equal to 3, 6, 9, 12, 15 and the fundamental periods, T_1 , of $0.1N$. Seismic demands of these frames under near-fault ground motions were obtained using the Open System for Earthquake Engineering Simulation (OpenSees) [10]. The main characteristics of these models can be found in references 8 and 9. Non-linear behavior of the frames was modeled by using rotational springs at the beam ends and at the bottom of the first-storey columns. Peak oriented hysteretic model and the energy based deterioration model was used to represent the non-linear load-deformation behavior of abovementioned rotational springs [11].

3 NEAR-FAULT PULSE-LIKE GROUND MOTIONS DATABASE

Increasing number of recorded near-fault ground motions, with seismologists and engineers efforts, may do recognizing those characteristics of this type of motions that strongly affect the dynamic responses of structures [12-14]. These researches have been generally focused on the pulse motions contained in near-fault records due to forward directivity and the fling step effects.

Considering that the pulse motions in near-fault records strongly affect the dynamic responses of structures [15], a large variability in the seismic demands of structures under scaled pulse-type motions may be observed, unless an appropriate method is used to scale this type of ground motions. Therefore, this study focused on a database of 40 near-fault earthquake records compiled from records that exhibit intense velocity pulses. The database includes the acceleration time-histories of the 2003 Bam (Bam station), the 1998 Golbaft (Sirch station), the 1990 Rudbar (Abbar station), the 1978 Tabas (Tabas station) and the 1977 Naghan (Naghan station) Iranian near-fault pulse-like earthquakes that were taken from Iran strong motion network data bank [16]. Moreover, 35 near-fault records, having distinct velocity pulses, were

taken from PEER strong motion database and added to this database [17]. All ground motions have been recorded on stiff soil, very dense soil and rock based on the ASCE7-10 [18] site classification for all faulting styles. The earthquake magnitude, M_w , ranges from 6.2 to 7.2, and the closest distance to fault rupture ranges from 0.07 to 18.2 km.

Near-fault ground motions have orientation that is controlled by the geometry of the fault, and thereby it is necessary to treat them as a vector rather than scalar quantities [19]. In this paper, 40 near-fault ground motion records were rotated to the fault-normal and fault-parallel components using the transformations proposed by Somerville [19]. Owing to more severity of the fault-normal components relative to the fault-parallel components [14], the normal components of the records were used as the seismic input in this study. It is worth noting that the pulse period and the peak spectral velocity of the used fault-normal components respectively range from 0.45 to 8.93 (*sec*), and from 84 to 500 (*cm/sec*).

4 DEVELOPMENT OF AN IMPROVED SCALING METHOD

Intensity measures (IM) are intermediate quantities which describe earthquake strength in terms of parameters that can be strongly related to seismic demands of structures. The pseudo spectral acceleration at the first period of a structure, $S_a(T_1)$, which is commonly used as the IM, may not show satisfactory correlation with the seismic demands distribution, particularly under near-fault pulse-like ground motions [5, 6]. This brought about as a result of two flaws of $S_a(T_1)$; one flaw is that this parameter does not describe the frequency content of ground motions at higher modes of vibration; and the other one is that it does not account for inelastic lengthening of modal periods as a structure softens under stiffness degradation. When the input time history is a near-fault pulse, these shortcomings are accentuated due to the sharp change in spectral ordinates around the pulse period [5].

In this study, in an attempt to compensate for the shortcomings of $S_a(T_1)$, a new improved scaling parameter was developed on the basis of the root-mean-square (RMS) value of spectral responses over the period range of $[T_a, T_b]$ in accordance with the following equation:

$$(S_{res})_{rms} = \left[\frac{1}{n} \sum_{i=1}^n S_{res}^2(T_i) \right]^{0.5}, \quad T_a \leq T_i \leq T_b \quad (1)$$

$$T_{i+1} = T_i + \Delta T$$

In Equation 1, $S_{res}(T_i)$ is the spectral response at T_i , and ΔT is equal to 0.025 (*sec*) for the 3-storey frame and 0.05 (*sec*) for other frames.

In developing this new improved IM according to Equation 1, there are two important key issues that should be carefully accounted in order to achieve the minimum amount of variability in seismic demands; firstly, which type of response spectrum (i.e. pseudo acceleration, velocity or displacement) is more capable to be used for calculating the root-mean-square value. In other words, which one of the parameters of $(S_a)_{rms}$, $(S_v)_{rms}$ and $(S_d)_{rms}$ is more efficient; secondly, with respect to the first mode period of a structure, which period range is more appropriate to be used for calculating the RMS value as improved IM.

4.1 Evaluation of the efficiency of the $(S_a)_{rms}$, $(S_v)_{rms}$ and $(S_d)_{rms}$ as the IM

Incremental dynamic analyses (IDAs) of the genetic frames under the near-fault ground motions were employed to determine the type of the response spectrum and the period range that can be reliably used to calculate the RMS value according to Equation 1. IDAs for the peak maximum interstory drift ratio, IDR_{max} , of the 6-storey and 12-storey frames in terms of $S_a(T_1)$ as the IM, are shown in Figure 1. Each point in these figures corresponds to the IDR_{max}

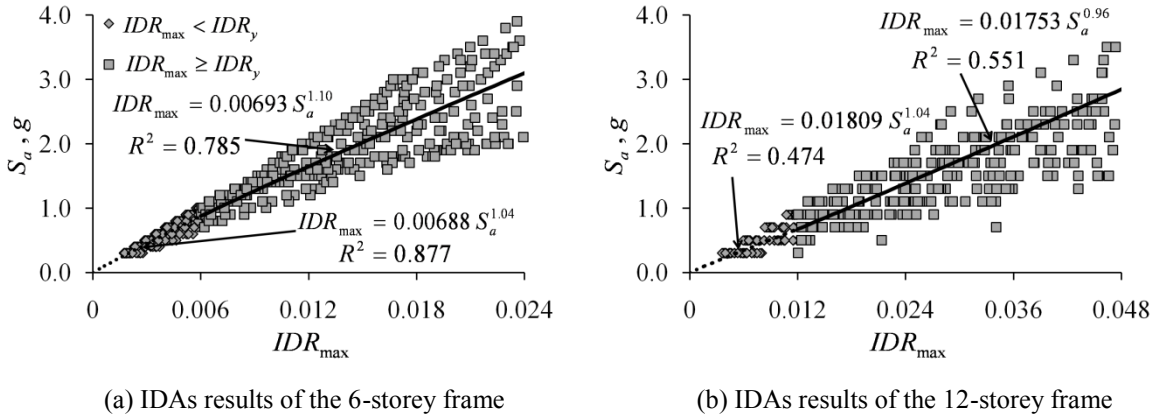


Figure 1: IDAs results of the 6 and 12-storey frames in terms of $S_a(T_1)$

of the frame obtained from a nonlinear dynamic analysis under a record scaled to a specific level of intensity.

The variability in IDAs can be quantified in terms of Coefficient Of Variation (COV) of IM values corresponding to a specific level of response (conditioned on a specific value of IDR_{max}) which was characterized by $COV_{(IM|IDR_{max})}$. The average value of $COV_{(IM|IDR_{max})}$ on the interval $[0, IDR_c]$ was calculated as the mean COV of the IM values, where IDR_c is the individual drift ratio capacities of the frames.

To select the best type of response spectrum for development of the improve IM, all possible period ranges of $[T_a, T_b]$ were used to calculate each of the parameters of $(S_a)_{rms}$, $(S_d)_{rms}$ and $(S_v)_{rms}$ as the alternative for IM. For each one of these alternatives, and based on the IDAs of the frames, the mean COV was calculated. The minimum amount of mean COV that can be achieved by using each of the parameters of $(S_a)_{rms}$, $(S_d)_{rms}$ and $(S_v)_{rms}$ was determined, which is provided in Figure 2.

Figure 2 indicates that the efficiency of $(S_a)_{rms}$, $(S_v)_{rms}$ and $(S_d)_{rms}$ is approximately similar for the 9 and 12-storey frames; however, $(S_a)_{rms}$ becomes more capable as the number of stories decreases to 3 and 6 or as it increases to 15. Based on these observations, velocity-based improved intensity measures are only appropriate for the 9, 12 and 15- storey frames included in the relatively low to moderate frequency systems. Therefore, with respect to the efficiency of $(S_a)_{rms}$ for all ranges of structural height, the parameter of $(S_a)_{rms}$ is chosen as the best estimation of an earthquake strength.

4.2 Selection of the optimal period range in order to reduce the overall variability

Relation of the mean COV to the period range of $[T_a, T_b]$ over which the parameter of $(S_a)_{rms}$ has been calculated according to Equation 1, is respectively shown in Figures 3a and 3b for the 6 and 12- storey frames, for instance. In these figures, the abscissa represents the ratio of T_a to T_1 and the ordinate represents the ratio of T_b to T_1 , where T_a and T_b are the lower and upper limits of the period range of $[T_a, T_b]$, and T_1 is the individual fundamental periods of the frames. The optimal period range, leading to the minimum mean COV, can be found from these figures, which strongly depends on the fundamental period of the frames as follows:

Optimal period range for short-period frames: Studying the relation of the mean COV to the period range for the 3 and 6-storey frames, which is presented in Figure 3a for the 6-storey frame as an example, reveals that the minimum scatter in the IDAs of short-period frames can be obtained by using the optimal period range of $[0.9T_1, 1.3T_1]$, among all period ranges. This implies that the period elongation effects in the seismic demand prediction of short-period

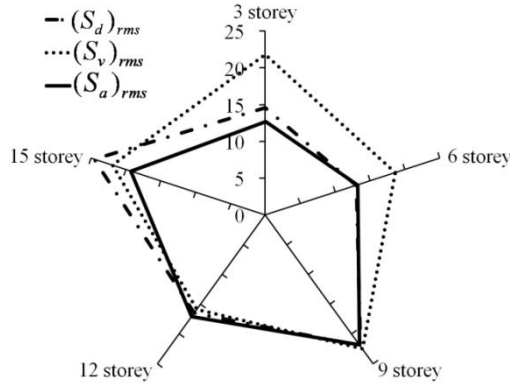
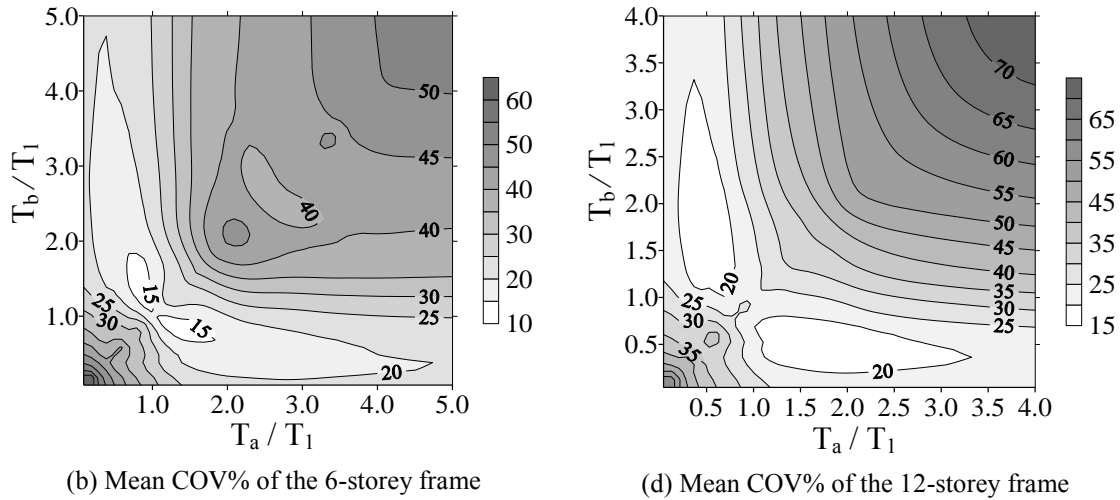


Figure 2: Minimum value of mean COV% in IDAs using $(S_a)_{rms}$, $(S_d)_{rms}$ and $(S_v)_{rms}$, calculated over the respective optimal period range



(b) Mean COV% of the 6-storey frame

(d) Mean COV% of the 12-storey frame

Figure 3: Mean COV% in IDAs results for $(S_a)_{rms}$ calculated over various period ranges of $[T_a, T_b]$

frames are significant, whereas the higher modes effects are insignificant.

Optimal period range for moderated to relatively long-period frames: Studying the results of the statistical evaluation shows that in addition to the effects of period elongation on the seismic demands of the 9, 12 and 15-storey frames, the effects of higher modes are also significant in these frames. Therefore, both higher modes effects and period elongation effects emerge in the optimal period range for these frames. Based on the mean COV values for the 9, 12 and 15-storey frames, which is presented in Figure 3b for 12-storey frame as an example, the minimum scatter in the IDAs of moderate to relatively long-period frames can be obtained by using the optimal period range of $[0.3T_1, 1.9T_1]$. It is worth nothing that considering the modal periods of the 9, 12 and 15-storey frames shows that the lower limit of the optimal period range (i.e. $0.3T_1$) is approximately equal to the average value of the T_2 and T_3 , where T_2 and T_3 are respectively the second and the third mode periods of the frame.

5 COMPARING THE EFFICIENCY OF $(S_A)_{RMS}$ AND $S_A(T_1)$

When performing IDAs of a structure under an ensemble of ground motions, a fraction of Ground Motions (GMs) will result in collapse of the structure at any given intensity level. Therefore, seismic demand prediction requires statistical response evaluation of the non collapse data (denoted NC) as well as the collapse data (denoted C) in accordance with the following equation [5]:

$$P[IDR_{max} > x | IM = im] = P[IDR_{max} > x | IM = im, NC] \cdot (1 - P_{C|IM=im}) + P_{C|IM=im} \quad (2)$$

where $P[IDR_{max} > x | IM = im, NC]$ is the probability of IDR_{max} exceeding a given level x at a given intensity level of im , for non-collapse data; and $P_{C|IM=im}$ is the probability of collapse at each im level. It should be mentioned that the collapse data (denoted C) was indicated by either non-convergence of dynamic analysis or excessive IDR_{max} demand in this study.

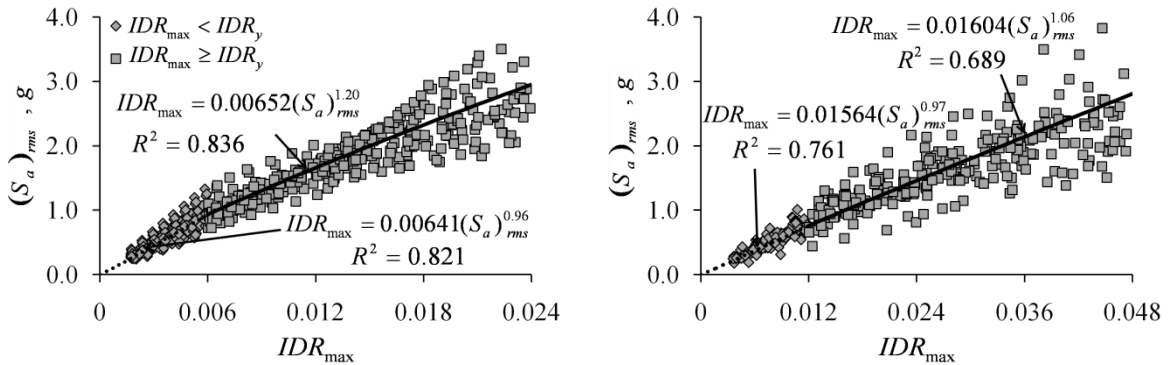
To improve the accuracy of seismic demand prediction in accordance with Equation 2, the improved IM should be able to reduce the variability in the non-collapse data as well as the collapse data, which will be discussed in the following for $S_a(T_I)$ and $(S_a)_{rms}$.

IDAs of short-period frames: Incremental dynamic analyses results of the 3 and 6-storey frames were adapted for the new improved IM of $(S_a)_{rms}$, calculated over the optimal period range of $[0.9T_I, 1.3T_I]$, in order to compare the efficiency of this new parameter with the commonly used parameter of $S_a(T_I)$. Non-collapse IDAs results of the 6-storey frame, presented in terms of $S_a(T_I)$ in Figure 1a, are provided in terms of $(S_a)_{rms}$ in Figure 4a as the example for IDAs of short-period frames. From comparing these figures, following observations can be made; for low levels of intensity at which the response is elastic the parameter of $(S_a)_{rms}$ results in more variability than $S_a(T_I)$. This follows the fact that linear responses of the short-period frames are dominated by the first mode of vibration. As the intensity of GMs is increased, period elongation effects become significant, and $(S_a)_{rms}$ provides more accurate estimation of responses. Using the optimal period range for calculating $(S_a)_{rms}$ made possible to significantly reduce the dispersions at large intensities so as not to substantially increase the scatter at low levels of intensity, and consequently the overall variability can be reduced.

Based on the non-collapse IDAs results (as shown in Figures 1a and 4a for the 6-storey frame), the overall variability was quantified in terms of dispersion of drift response conditioned on the ground motion intensity measure. For this purpose, dispersion was calculated according to the following equation as the standard deviation of the drift data from an average response curve obtained from regression analysis between drift and the seismic intensity:

$$\sigma_{IDR_{max}} = \left[\sum_{i=1}^n (IDR_{max,i} - \widehat{IDR}_{max,i})^2 / (n - 1) \right]^{1/2} \quad (3)$$

In Equation 3, $IDR_{max,i}$ is the i th response obtained from a nonlinear dynamic analysis under a record scaled to a specific level of intensity, $\widehat{IDR}_{max,i}$ is the average response obtained from regression curve at the same intensity for which $IDR_{max,i}$ was calculated, and n is the sample size of the non-collapse data at all levels of intensity (as an example for the 6-storey frame, n is the number of points in Figures 1a or 4a).



(a) IDAs results of the 6-storey frame

(b) IDAs results of the 12-storey frame

Figure 4: IDAs results of the 6 and 12-storey frames in terms of $(S_a)_{rms}$

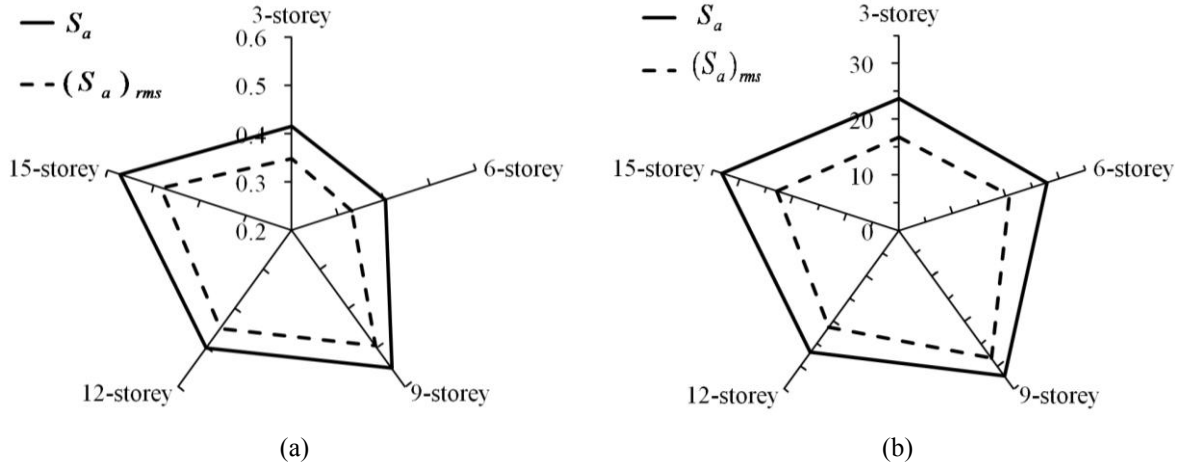


Figure 5: (a) The ratio of the standard deviation to IDR_y for IDAs results of the frames based on $S_a(T_I)$ and $(S_a)_{rms}$, (b) COV% in the IM values leading to collapse for $S_a(T_I)$ and $(S_a)_{rms}$

Figure 5a provides the ratio of the standard deviation, which was calculated in accordance with Equation 3, to the individual yield drift ratios of frames (i.e. $\sigma_{IDR_{max}}/IDR_y$), for all frames and for $S_a(T_I)$ and $(S_a)_{rms}$. It can be seen that $(S_a)_{rms}$ can respectively reduce the $\sigma_{IDR_{max}}/IDR_y$ of the 3 and 6-storey frames from 0.42 and 0.40 for $S_a(T_I)$ to 0.35 and 0.33, and in so doing can improve the accuracy of the non-collapse seismic demand prediction (i.e. $P[IDR_{max} > x|IM = im, NC]$ in Equation 2).

While $(S_a)_{rms}$ reduces the overall dispersion, this reduction is most apparent at larger drifts, where the structure behaves nonlinearity. This implies that in addition to improvement of the accuracy in predicting the non-collapse seismic demand, $(S_a)_{rms}$ can increase the accuracy of collapse capacity prediction. The intensity (IM value) at which structural collapse is occurred under an earthquake record, is referred to as collapse capacity of the structure under the earthquake record. The considerable difference between the efficiency of $S_a(T_I)$ and $(S_a)_{rms}$ in collapse capacity prediction of the 3 and 6-storey frames, can be clearly observed in Figure 5b. From this figure, it can be observed that the COV in the IM values leading to collapse of the 3 and 6-storey frames were respectively reduced from 23.7 and 27.8 percent for $S_a(T_I)$ to 16.8 and 20.8 percent for $(S_a)_{rms}$. Therefore, the parameter of $(S_a)_{rms}$ can considerably improve the accuracy of the collapse prediction of the short-period frames (i.e. $P_{C|IM=im}$ in Equation 2).

IDAs of moderate to relatively long-period frames: Non-collapse IDA results of the 12-storey frame, presented in terms of $S_a(T_I)$ in Figure 1b, are provided in terms of $(S_a)_{rms}$ in Figure 4b as the example for the IDAs of moderate to relatively long-period frames. It should be mentioned that for these frames, $(S_a)_{rms}$ was calculated over the optimal period range of $[0.3T_I, 1.9T_I]$. From Figures 1b and 4b, it can be observed that R^2 factor, an indicator of how well the equation resulting from the regression analysis, is significantly increased from 0.474 for $S_a(T_I)$ to 0.761 for $(S_a)_{rms}$ at low levels of response ($IDR_{max} < IDR_y$), and from 0.551 for $S_a(T_I)$ to 0.689 for $(S_a)_{rms}$ at high levels of response ($IDR_{max} > IDR_y$), where IDR_y is the yield interstorey drift ratio of the frame.

The ratio of $\sigma_{IDR_{max}}/IDR_y$ was calculated according to Equation 3 for non-collapse IDAs results of the 9, 12 and 15-storey frames for $S_a(T_I)$ and $(S_a)_{rms}$, which is shown in Figure 5a. This figure demonstrates that $(S_a)_{rms}$ can considerably reduce the $\sigma_{IDR_{max}}/IDR_y$, and thereby can enhance the accuracy of the non-collapse seismic demand prediction. In addition to the ability in non-collapse seismic demand prediction, $(S_a)_{rms}$ can be efficiently employed in predicting the probability of collapse. The COV in collapse capacities of the 9, 12 and 15-storey frames for $S_a(T_I)$ and $(S_a)_{rms}$ are presented in Figure 5b. This figure implies that using $(S_a)_{rms}$

can respectively reduce the COV in collapse prediction of the 9, 12 and 15-storey frames from 32.1, 26.9 and 33.3 percent for $S_a(T_I)$ to 28.2, 21.4 and 23.0 percent. Reduction in the dispersion of non-collapse data as well as the collapse data in this way helps reducing the number of records necessary to predict the probability that seismic demand exceeds a given value, in accordance with Equation 2, within a specified confidence interval.

6 CONCLUSION

With the goal of developing an improved intensity measure (IM) for scaling near-fault pulse-like ground motions, the ability of root-mean-square (RMS) of spectral responses, calculated over the optimal period range, was considered in this study. The evaluation of RMS of spectral responses has led to the following conclusions:

1. It was concluded that root-mean-square of pseudo spectral accelerations, $(S_a)_{rms}$ generally provides much superior results with respect to those of spectral displacements, $(S_d)_{rms}$, and spectral velocities, $(S_v)_{rms}$.
2. Statistical evaluations of IDAs results of the 3 and 6-storey frames, short-period frames, revealed that calculating the $(S_a)_{rms}$ over the optimal period range of $[0.9T_I, 1.3T_I]$, compared to all possible period ranges, was led to the minimum overall variability in the predicted seismic demands. This illustrates the significance of period elongation effects in seismic demand prediction of short-period frames through incremental dynamic analyses.
3. Based on the statistical evaluation of IDAs results of the 9, 12 and 15-storey frames, moderated to relatively long-period frames, it was concluded that the minimum overall scatter in the IDAs results can be obtained by using the optimal period range of $[0.3T_I, 1.9T_I]$, among all possible period ranges. This indicated that both higher modes effects and period elongation effects are significantly important in seismic demand prediction of these frames in terms of $(S_a)_{rms}$.
4. The seismic intensity scaling index of $(S_a)_{rms}$, calculated over the optimal period, compared to $S_a(T_I)$ can considerably reduce the $\sigma_{IDR_{max}}/IDR_y$, the ratio of the standard deviation of non-collapse IDR_{max} demands to the individual yield IDR of the frames. By using $(S_a)_{rms}$, the ratio of $\sigma_{IDR_{max}}/IDR_y$ for the 3, 6, 9, 12 and 15-storey frames was respectively reduced by the relative amount of 16, 18, 10, 10 and 15 percent compared to those of $S_a(T_I)$.
5. The newly proposed IM can also reduce the dispersion in predicted collapse capacities of the frames by the relative amount of 24 percent compared to $S_a(T_I)$ on average.

REFERENCES

- [1] D. Vamvatsikos, C.A. Cornell, Incremental dynamic analysis. *Earthq. Eng. Struct. Dynam.*, **31**(3), 491-514, 2002a.
- [2] J.R. Benjamin, C.A. Cornell, *Probability, Statistics, and Decision for Civil Engineers*, McGraw Hill, 1970.
- [3] E. Kalkan, S.E. Kunnath, Effects of fling step and forward directivity on seismic response of buildings. *Earthq. Spectra*, **22** (2), 360-390, 2006.
- [4] J.W. Baker, C.A. Cornell, A vector-valued ground motion intensity measure consisting of spectral acceleration and epsilon. *Earthq. Eng. Struct. Dynam.*, **34**(10), 1193-1217, 2005.

- [5] P. Tothong, C.A. Cornell, Probabilistic seismic demand analysis using advanced ground motions intensity measures, attenuation relationships, and near-fault effects, Report 2006/11, Pacific Earthquake Engineering Research Center, Berkeley, CA, 2007.
- [6] J.W. Baker, C.A. Cornell, A vector-valued ground motion intensity measures for pulse-like near-fault ground motions. *Eng. Struct.*, **30**(4), 1048-1057, 2008.
- [7] D. Yang, J. Pan, G. Li, Non-structure-specific intensity measures parameters and characteristics of near-fault ground motions. *Earthq. Eng. Struct. Dynam.*, **38**(11), 1257 – 1280, 2009.
- [8] A. Yahyaabadi, M. Tehranizadeh, Nonlinear dynamic analysis of structures under near-fault ground motions using an improved scaling method. *Asian Journal of Civil Engineering*, **11**(5), 627-643, 2010.
- [9] R. Medina, H. Krawinkler, Seismic Demands for Nondeteriorating Frame Structures and Their Dependence on Ground Motions, Report No. PEER 2003/15, Pacific Earthquake Engineering Research Center, Berkeley, CA, 2004.
- [10] OpenSees, Open System for Earthquake Engineering Simulation, Pacific Earthquake Engineering Research Center, Berkeley, CA, 2009.
- [11] L.F. Ibarra, R.A. Medina, H. Krawinkler, Hysteretic models that incorporate strength and stiffness deterioration. *Earthq. Eng. Struct. Dynam.*, **34**(12), 1489-1511, 2005.
- [12] P.G. Somerville, R. Graves, Conditions that give rise to unusually large long period ground motions. *Struct. Des. Tall Spec.*, **2**(3), 211-232, 1993.
- [13] J.D. Bray, A. Rodriguez-Marek, Characterization of forward-directivity ground motions in the near-fault region. *Soil Dyn. Earthq. Eng.*, **24**(11), 815-828, 2004.
- [14] E. Chioccarelli, I. Iervolino, Near-source seismic demand and pulse-like records: A discussion for L Aquila earthquake. *Earthq. Eng. Struct. Dynam.*, **39**(9), 1039-1062, 2010.
- [15] H. Krawinkler, B. Alavi, F. Zareian, Impact of near-fault pulses on engineering design. *Direction in Strong Motion Instrumentation*, **58**(2), 83-106, 2005.
- [16] Iran Strong Motion Network Data Bank, <http://www.bhrc.ac.ir>
- [17] PEER Strong Ground Motion Database, <http://peer.berkeley.edu/smcat/>
- [18] American Society of Civil Engineering, ASCE7-10: Minimum Design loads for buildings and other structures. Reston, Virginia, 2010.
- [19] P.G. Somerville, Characterizing near fault ground motion for the design and evaluation of bridges. *Third National Seismic Conference and Workshop on Bridges and Highways*, Portland, Oregon, 2002.